Progress In Electromagnetics Research, PIER 102, 95–106, 2010

COMPACT, BROAD-STOPBAND LOWPASS FILTERS USING SIRS-LOADED CIRCULAR HAIRPIN RESONATORS

M. H. Yang, J. Xu, Q. Zhao, L. Peng, and G. P. Li

Institute of Applied Physics
University of Electronic Science and Technology of China
Chengdu 610054, China

Abstract—A novel compact resonator for LPF is proposed in this paper. It is composed of a circular hairpin resonator and a pair of coupled parallel stepped impedance resonators (SIRs) inside. With the loaded SIRs, additional two transmission zeros can be introduced and adjusted easily to cancel the spurious responses for stopband extending, while do not change the filter size. Filters using one and two of the new cells were designed and measured. The two-cell LPF has an insertion loss less than 0.6 dB from DC to 1.6 GHz, including attenuation of double SMA transitions at both sides of the circuit which is about 0.3 dB and a wide −10 dB stopband from 2.5 to 13 GHz (corresponding to 146% normalized 10 dB stopband), but has a size of only $0.129\lambda g \times 0.073\lambda g$.

1. INTRODUCTION

Lowpass filters are widely used in microwave circuits to suppress unwanted harmonics and spurious bands. However, conventional stepped-impedance and *L-C* ladder type LPFs not only have large sizes but also have narrow stopband and gradual cutoff frequency responses [1], which usually restrict their application ranges. Therefore, compact size and wide-stopband LPFs are required. For a filter using conventional resonators, to get a sharper roll-off, numbers of sections will be needed but at the cost of increased sizes and insertion losses. To get wide stopband and sharp roll-off responses, many new methods have been proposed, such as defected ground structure (DGS) [2–9] and electromagnetic band-gap (EBG) [10–13]. However, as we know, the etched ground of the DGS and periodic character of the EBG will cause radiation and larger size problems, respectively. As an

Corresponding author: M. H. Yang (yangmaohui@uestc.edu.cn).

elliptic-function LPF can introduce finite-frequency attenuation poles to improve its cutoff frequency responses, it is frequently used in many microwave circuits. Since conventional elliptic-function LPFs usually have larger sizes and narrow stopband [1], filter designers prefer to propose different types of compact microstrip resonators (CMRCs) with quasi-elliptic-function characters for LPF in the past few years, such as spiral compact microstrip resonator cell (SCMRC) [14–16], which has a restricted 10 dB stopband less than 40% using one cell and more than 90% 10 dB stopband using five cells. An in-line beeline CMRC was proposed in [17], and the three-cell LPF achieved a 10 dB bandwidth of 128%. Later, another kind of LPF CMRC was studied in [18], which has a sharp cutoff roll-off, a 10 dB stopband of 138.3% and a normalized length about $0.23\lambda g$. However, its asymmetrical configuration may cause design difficulties. Recently, two new types of CMRCs have been reported in [19] and [20]. Their measured results show that the two four-cell filters have 10 dB stopband of 135% and 152%, and normalized circuit lengths amount to $0.35\lambda g$ and $0.62\lambda g$, respectively.

Among those proposed resonators, capacitor coupling hairpin cells have been widely used since the first LPF was reported in 2001 [21]. The six-cell filter provides a 10 dB stopband more than 135% with a sharp roll-off and flat stopband attenuation, and its normalized length was minimized to $0.37\lambda g$ [22]. Recently, a new LPF which has a structure similar to hairpin resonator has been reported in [23]. The LPF has a relative stopband of 104% and a normalized circuit size of $0.16\lambda g \times 0.14\lambda g$. However, the passband insertion loss seems high. In our previous work, a SIRs-loaded hairpin cell used for LPF was studied [24]. The filter was compact and had a wide stopband, but an obvious ripple still existed. Because the physical sizes of the added parallel SIRs are restricted by the spare space within the hairpin resonator, the introduced transmission zeros can only be adjusted within a narrow range, so the ripple may not be absolutely eliminated. To solve this problem, a new type of circular SIRs-loaded hairpin resonator cell is proposed, as shown in Fig. 1. Compared with the resonator in [24], it has a merit that the transmission zeros in the stopband can be tuned easily in a wide range, and the ripple can be completely eliminated without increasing the size of the whole structure. Therefore, the stopband characteristics will be more controllable. Besides, the impedance of the feed line matches better with that of circular resonator than the conventional hairpin resonator case. This will be illustrated in the following frequency response curves. The equivalent LC circuit and values of the circuit's parameters are also presented in this paper.

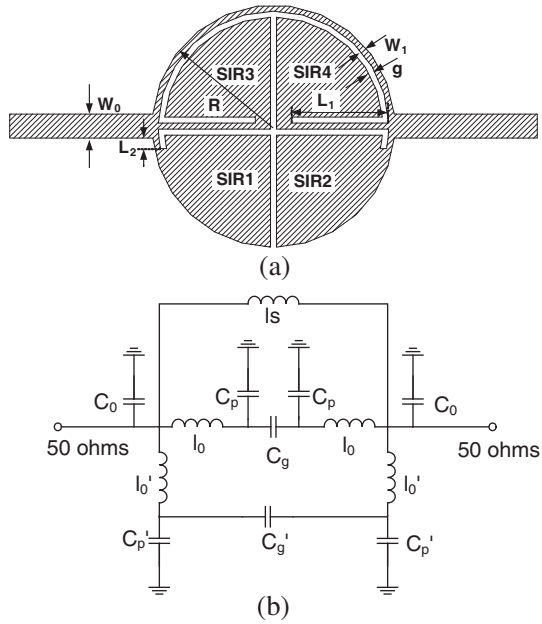

Figure 1. One-cell LPF using the new resonator cell. (a) Layout. (b) Equivalent circuit.

To validate the availability of the new resonator, two filters using one and two of the new cells were fabricated and tested. The one-cell LPF has a 3 dB cutoff frequency at 2 GHz and a 10 dB stopband from 2.5 to 8.3 GHz, and corresponding 107% normalized 10 dB stopband is achieved, while has a size of only $0.073\lambda g \times 0.073\lambda g$, where λg is the guide-wavelength at the 3 dB cutoff frequency 2 GHz. The two-cell LPF has a wide 10 dB stopband from 2.5 to 13 GHz, and corresponding 146% normalized 10 dB bandstop is achieved, while has a size of $0.129\lambda g \times 0.073\lambda g$. The maximal attenuation in the stopband of the two-cell LPF can reach 70 dB. With the advantages of compact size, wide stopband, and low insertion loss, this type of filters could be used widely in many microwave circuits.

2. ONE-CELL FILTER DESIGN

Figure 1(a) shows the layout of the one-cell LPF which is composed of the proposed resonator and two direct-connect 50 Ω feed lines. In distributed filter design, most designers might try to deduce the ABCD matrixes of the filters and get the accurate frequency responses of the

circuits. However, the transmission matrix of the new filter is too complicated to determine the corresponding physical dimensions. So, in order to better understand the characteristics of the new filter, the equivalent LC circuit will be discussed in this paper.

2.1. LC Parameters Extraction

Figure 1(b) is the equivalent LC circuit of the filter. l_s is the inductance introduced by the upper narrow line with width W_1. l_0, l_0' are the inductances introduced by l_1 and l_2, respectively. C_g is the coupling capacitor between SIR3 and SIR4. C_g' is the coupling capacitor between SIR1 and SIR2. C_p and C_p' are the metal-insulator-metal (MIM) capacitors introduced by SIR1 to 4. C_0 is the sum of the capacitances of the junction discontinuities between the main feed line and three narrow inductance lines. The values of those parameters can be extracted using the methods discussed in [1], and they are summarized here. A high-impedance lossless line terminated at both ends by relatively low impedance lines can be presented by a π-equivalent circuit, as shown in Fig. 2(a).

The values of l_s and c_s can be obtained as

$$l_s = \frac{1}{w} \times Z_s \times \sin\left(\frac{2\pi}{\lambda_g} l\right) \tag{1}$$

$$C_s = \frac{1}{w} \times \frac{1}{Z_s} \times \tan\left(\frac{\pi}{\lambda_g} l\right), \tag{2}$$

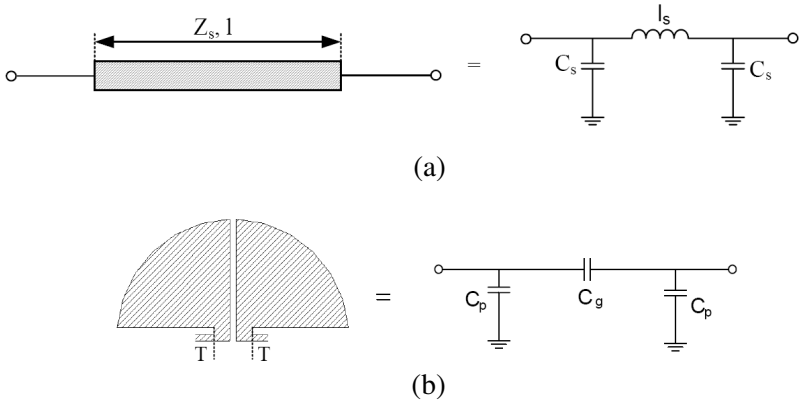

Figure 2. Microstrip circuits and equivalent LC circuits. (a) Inductance microstrip line. (b) Coupled microstrip lines.

where Z_s is the characteristic impedance of the line. l is the length of it, and λ_g is the guided wavelength at the cutoff frequency. The values of the capacitors introduced by the coupled lines (as shown in Fig. 2(b)) can be extracted using an EM simulator, for the EM simulator not only can simulate the filter without restricting of its physical parameters but also can calculate the capacitor including fringing capacitors. The values of C_g and C_p can be deduced by

$$C_g = \frac{-\mathrm{Im}(Y_{21})}{w_c} \tag{3}$$

$$C_p = \frac{\mathrm{Im}(Y_{11} + Y_{21})}{w_c}, \tag{4}$$

where w_c is the cutoff frequency of the LPF. Y_{11} and Y_{22} are the simulated admittance parameters of the coupled line, and $\mathrm{Im}(x)$ denotes the imaginary part of x. The note T represents the reference planes. C_p and C'_p can also be extracted by the same process.

2.2. Characteristics of the New LPF

In order to better understand the characteristics of the new filter, a demonstrated filter was designed. The filter was fabricated on 0.254 mm thick RT/Duroid 5880 substrate with a relative dielectric constant of 2.2, and parameters of the filter are $R = 4\,\mathrm{mm}$, $l_1 = 3.2\,\mathrm{mm}$, $l_2 = 0.23\,\mathrm{mm}$, $w_0 = 0.79\,\mathrm{mm}$ (corresponding to $50\,\Omega$ characteristic impedance). The widths of all the narrow inductance lines are set to $w_1 = 0.2\,\mathrm{mm}$, and the gaps are set to $g = 0.2\,\mathrm{mm}$. The equivalent LC parameters of the filter can be deduced using the method mentioned above, which are summarized in Table 1. All the simulations in this paper were accomplished using HFSS 10.0.

Table 1. Values of the extracted LC parameters of the one-cell filter (units: C, pF; L, nH).

Parameters	l_s	C_0	C_g	C_p	l_0	C'_g	C'_p	l'_0
Values	5.12	0.325	0.029	0.997	1.488	0.059	1.18	0.187

The new filter can be divided into two circular hairpin LPFs, as shown in Fig. 3. It should be mentioned that the transformation is not accurate because the transmission matrix cannot simply be divided into two parts. However, that will help us understanding its stopband characteristics, especially the positions of the transmission zeros. The equivalent LC circuit of filter a is shown in Fig. 3(c). It is a quasi-elliptic-function LPF [1]. The cutoff frequency is mainly determined

by the values of l_s and C_g, and the transmission zeros are mainly determined by the values of l_0 and C_p [1]. Since L_1 is longer than L_2, the corresponding inductance L_0 is much higher than L_0'. Therefore, SIR3 and SIR4, as added resonators, provide additional two zeros located at lower frequencies, and SIR1 and SIR2 at higher frequencies. The simulated results of the two filers are shown in Fig. 4, from which we can see that the new filter shown in Fig. 1 has a lower cutoff frequency and an improved stopband compared with filter a or filter b, but has the same length as both of them. From Fig. 4, one can also see that, for a single circular hairpin LPF (filter a or filter b), the pass-band return losses are greatly improved than the conventional capacitor coupling hairpin resonator [22, 24], so this perfect-impedance-matching circular hairpin resonators can also be used separately in some circuits.

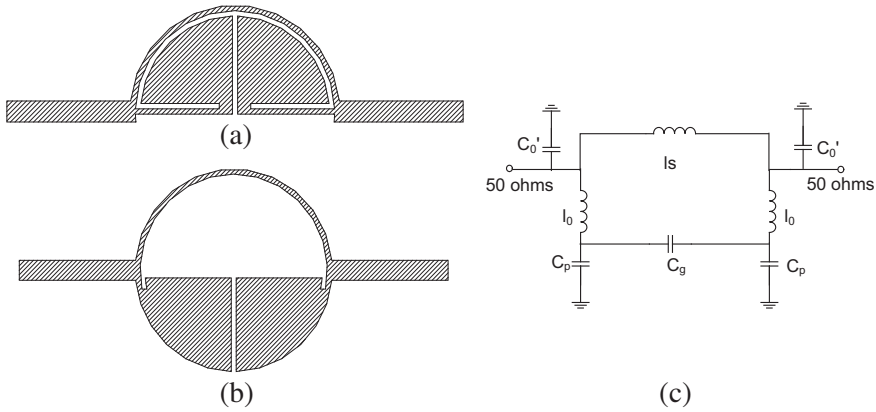

Figure 3. Layout of the circular hairpin LPFs. (a) Filter a. (b) Filter b. (c) Equivalent circuit of filter a.

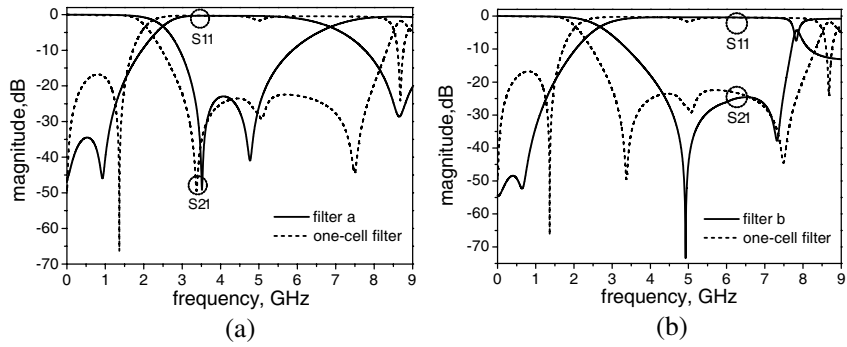

Figure 4. Simulated results of the filters. (a) Filter a and one-cell filter. (b) Filter b and one-cell filter.

2.3. Characters of the Transmission Zeros

In the new broad stopband filter design, the 3 dB cutoff frequency f_c can be tuned by changing R_0 values. When f_c is fixed, the next step is to adjust Z_2 and Z_3 to locate them at the first spurious frequency and to cancel it.

Figure 5 shows the simulated S parameters of the new filter with different l_1 and l_2 lengths. Decreasing L_1 length, when keep other parameters unchanged, Z_1, Z_2 move to high frequencies, while has negligible effects on the positions of f_c, Z_3, and Z_4 (as shown in Fig. 5(a)). On the other hand, increasing L_2 value, Z_3 and Z_4 are adjusted to be located at lower frequencies, while without having significant effect on f_c, Z_1, and Z_2 (as shown in Fig. 5(b)). To sum up, the first spurious response can be eliminated just through adjusting the length of L_1 or L_2 without changing the size of the whole filter, which greatly facilitates the design. Moreover, different stopband characteristics can also be obtained by putting the zeros at different frequencies.

Figure 6 shows the simulated and measured results of the fabricated filter. The first ripple at 5.1 GHz was compressed well, and the 3 dB stopband was extended to 8.2 GHz, four times the cutoff frequency f_c. The filter has a size of 8×8 mm, corresponding to $0.073\lambda g \times 0.073\lambda g$. In Fig. 6, the equivalent LC circuit was simulated using ADS. We found that the simulated responses of the LC circuits agree very well with the measured results. Though there are some discrepancies at high frequencies, it can be understood because the lumped LC circuit can only present the distribute circuit at the calculated frequency 2 GHz. The accuracy of the LC circuit has also been proved.

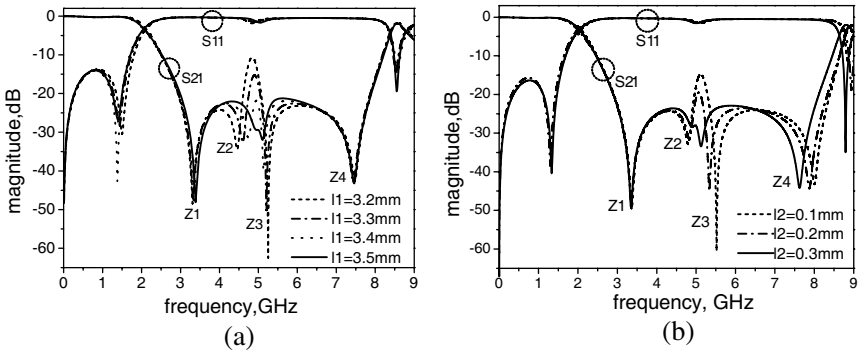

Figure 5. Simulated frequency responses of the new proposed LPF with different physical size. (a) With different l_1 lengths. (b) With different l_2 lengths.

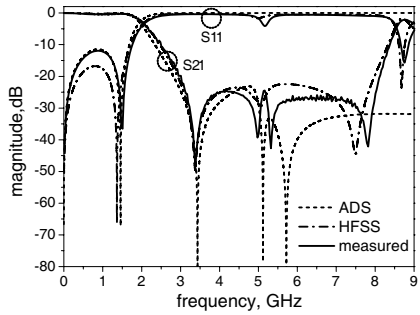

Figure 6. Simulated and measured S-parameters of the new LPF.

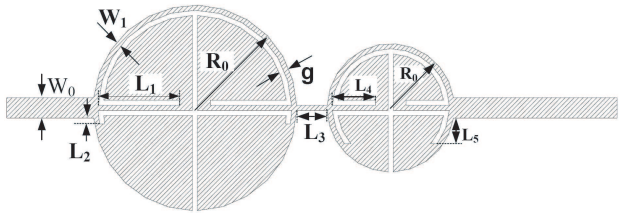

Figure 7. Layout of the proposed filter.

3. TWO-CELL FILTER DESIGN

To get an even broader stopband and strengthen the attenuation of the stopband, filters using several sections of the new cells can be adopted. Fig. 7 shows a LPF by cascading two SIRs-loaded circular resonators having different radii, corresponding to different cutoff frequencies and positions of transmission zeros. The two cells are connected by a short inductance line l_3 with a narrow width of W_1, and this method can be found in [25]. By properly putting the transmission zeros of the two filters at the desired frequencies, broad stopband can be obtained. Compared with conventional filers, which usually using uniform size resonators and nearly half wavelength transform lines between two connected resonators, the new filter will be more compact.

To validate the theory described above, a demonstrated filter was designed, fabricated and measured. It has dimensions as follows: $R_0 = 4\,\text{mm}$, $R_1 = 2.5\,\text{mm}$, $l_1 = 3.2\,\text{mm}$, $l_2 = 0.23\,\text{mm}$, $l_3 = 1.2\,\text{mm}$, $l_4 = 1.7\,\text{mm}$, $l_5 = 1\,\text{mm}$, $w_0 = 0.79\,\text{mm}$. Fig. 8 shows the simulated S parameters of the connected R_1-radius LPF. It has a 3 dB stopband from 4 to 12 GHz and two transmission zeros at 6.3 and 10.5 GHz. Fig. 9 shows the measured and simulated frequency responses of the

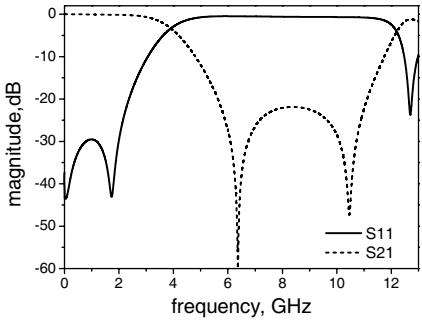

Figure 8. Simulated results of the R_1-radius LPF.

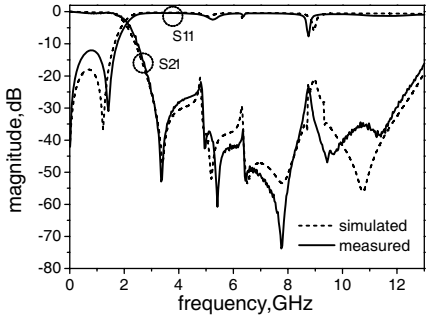

Figure 9. Simulated and measured results of the proposed two-cell LPF.

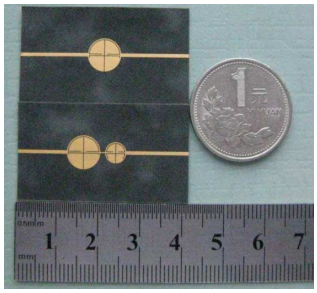

Figure 10. Photograph of the fabricated LPFs.

fabricated two-cell filter. The filter has an insertion loss less than 0.6 dB from DC to 1.6 GHz, including the attenuation of double SMA transitions at both sides of the test circuit which is about 0.3 dB. It has a return loss better than −10 dB covering from 2.5 to 16 GHz, and approximately 146% (−10 dB) bandwidth is obtained. The measured and simulated results agree very well. Fig. 10 shows the photograph of the fabricated two filters. The two-cell filter has a size of 14.2×8 mm, corresponding to $0.129\lambda g \times 0.073\lambda g$, where λg is guided wavelength at the cutoff frequency of 2 GHz. The two filters are very compact and have wide stopband and low insertion losses. They could be used widely in many microwave circuits.

4. CONCLUSION

A novel compact resonator cell for elliptic-function LPFs is proposed in this paper. One of the main features of the cell is that it can

introduce four transmission zeros in the stopband, and the positions of them can be tuned easily to get different stopband characteristics for different system requirements, while do not change the filter size. To apply this cell, two broad stopband LPFs using one and two of the new cells are designed, fabricated and tested. The two filters have very compact sizes, broad stopband, and low insertion losses. The equivalent *LC* circuit of this type of resonator is given, and values of the circuit's parameters are deduced. The simulated lumped circuit frequency responses agree very well with the measured results. High performance filters based on the novel resonators could find great potential applications in many microwave circuits.

REFERENCES

1. Hong, J. S. and M. J. Lancaster, *Microstrip Filters for RF/Mcirowave Applications*, Wiley, New York, 2001.
2. Mandal, M. K., P. Mondal, S. Sanyal, and A. Chakrabarty, "Low insertion-loss, sharp-rejection and compact microstrip low-pass filters," *IEEE Microwave and Wireless Components Lett.*, Vol. 16, No. 11, 600–602, 2006.
3. Castillo, M. D., V. Ahumada, J. Martel, and F. Medina, "Design of compact low-pass elliptic filters using double-sided MIC technology," *IEEE Trans. Micro. Theory Tech.*, Vol. 55, No. 1, 121–127, 2007.
4. Weng, L. H., S. J. Shi, X. Q. Chen, Y. C. Guo, and X. W. Shi, "A novel CSRRs DGS as lowpass filter," *Journal of Electromagnetic Waves and Applications*, Vol. 22, No. 14–15, 1899–1906, 2008.
5. Chen, H. and Y.-X. Zhang, "A novel and compact low-pass quasi-elliptic filter using hybrid microstrip/CPW structure," *Journal of Electromagnetic Waves and Applications*, Vol. 22, No. 17–18, 2347–2353, 2008.
6. Chen, X. Q., L. H. Weng, and X. W. Shi, "Equivalent circuit analyzed of complementary split ring resonator DGS for low pass filter," *Journal of Electromagnetic Waves and Applications*, Vol. 22, No. 17–18, 2365–2372, 2008.
7. Song, Q. Y., H. R. Cheng, X. H. Wang, L. Xu, X. Q. Chen, and X. W. Shi, "Novel wideband bandpass filer integrating HMSIW with DGS," *Journal of Electromagnetic Waves and Applications*, Vol. 23, 2031–2040, 2009.
8. Chen, W.-N., "A novel approach for realizing 2.4/5.2 GHz dual-band BPFs using twin-spiral etched ground structure," *Journal of Electromagnetic Waves and Applications*, Vol. 23, 829–840, 2009.

9. Chen, X.-Q., R. Li, S.-J. Shi, Q. Wang, L. Xu, and X.-W. Shi, "A novel low pass filter using elliptic shape defected ground structure," *Progress In Electromagnetics Research B*, Vol. 9, 117–126, 2008.
10. Yang, F. R., K. P. Ma, Y. X. Qian, and T. Itoh, "A uniplanar compact photonic-bandgap (UC-PBG) structure and its applications for microwave circuit," *IEEE Trans. Micro. Theory Tech.*, Vol. 47, No. 8, 1509–1514, 1999.
11. Chen, M., C.-Y. Jiang, W.-Q. Xu, and M.-H. Ho, "Design of high order suspended stripline bandpass filter with miniaturization," *Progress In Electromagnetics Research Letters*, Vol. 8, 9–17, 2009.
12. Shaban, H. F., H. A. Elmikaty, and A. A. Shaalan, "Study the effects of electromagnetic band-gap (EBG) substrate on two patch microstrip antenna," *Progress In Electromagnetics Research B*, Vol. 10, 55–74, 2008.
13. Karthikeyan, S. S. and R. S. Kshetrimayum, "Compact wideband bandpass filter using open slot split ring resonator and CMRC," *Progress In Electromagnetics Research Letters*, Vol. 10, 39–48, 2009.
14. Gu, J. and X. Sun, "Compact lowpass filter using spiral compact microstrip resonant cells," *IEE Electron. Lett.*, Vol. 41, No. 19, 1065–1066, 2005.
15. Peng, Y. and W.-X. Zhang, "Microstrip band-reject filter based on inter-digital capacitance loaded loop resonators," *Progress In Electromagnetics Research Letters*, Vol. 8, 93–103, 2009.
16. Hejazi, Z. M., M. C. Scardelletti, F. W. van Keuls, A. A. Omar, and A. S. Al-Zayed, "EM full-wave analysis and testing of novel quasi-elliptic microstrip filters for ultra narrowband filter design," *Progress In Electromagnetics Research*, PIER 85, 261–288, 2008.
17. Zhang, F., J. Z. Gu, C. Y. Gu, L. N. Shi, C. F. Li, and X. W. Sun, "Lowpass filter with in-line beeline CMRC," *IEE Electron. Lett.*, Vol. 42, No. 8, 472–474, 2006.
18. Deng, K., Q. Xue, and W. Che, "Improved compact microstrip resonance cell lowpass filter with wide stopband characteristics," *IEE Electron. Lett.*, Vol. 43, No. 8, 463–464, 2007.
19. Li, J.-L., S.-W. Qu, and Q. Xue, "Compact microstrip lowpass filter with sharp roll-off and wide stop-band," *IEE Electron. Lett.*, Vol. 45, No. 2, 110–111, 2009.
20. Li, L., Z.-F. Li, and Q.-F. Wei, "Compact and selective lowpass filter with very wide stopband using tapered compact microstrip resonant cells," *IEE Electron. Lett.*, Vol. 45, No. 5, 267–268, 2009.

21. Hsieh, L. H. and K. Chang, "Compact lowpass filter using stepped impedance hairpin resonator," *IEE Electron. Lett.*, Vol. 37, No. 4, 899–900, 2001.
22. Hsieh, L. H. and K. Chang, "Compact elliptic-function low-pass filters using microstrip stepped-impedance hairpin resonators," *IEEE Trans. Micro. Theory Tech.*, Vol. 51, No. 1, 193–199, 2003.
23. He, Q. J. and C. J. Liu, "A novel low-pass filter with an embedded band-stop structure for improved stop-band characteristics," *IEEE Trans. Micro. Theory Tech.*, Vol. 19, No. 10, 629–631, 2009.
24. Yang, M. H. and J. Xu, "Design of compact, broad-stopband lowpass filter using modified stepped impedance hairpin resonators," *IEE Electron. Lett.*, Vol. 44, No. 20, 899–900, 2008.
25. Luo, S., L. Zhu, and S. Sun, "Stopband-expanded low-pass filters using microstrip coupled-line hairpin units," *IEEE Microwave and Wireless Components Lett.*, Vol. 18, No. 8, 506–508, 2008.